Quantifying CBF from Arterial Spin Labeling via Diverse-TI: sampling diversity or repetitions?

Lei Yu, Pierre Maurel, Christian Barillot, Rémi Gribonval

Quantifying CBF from Aterial Spin Labeling via Diverse-TI: sampling diversity or repetitions ?

Lei Yu, Pierre Maurel, Christian Barillot, Remi Gribonval

Quantifying CBF from Aterial Spin Labeling via Diverse-TI: sampling diversity or repetitions ?

Lei Yu[*†‡§], Pierre Maurel[†‡§*], Christian Barillot[†‡§*], Remi Gribonval[*]

Project-Team Visages

Abstract: Arterial Spin Labeling (ASL) is a noninvasive perfusion technique which allows the absolute quantification of Cerebral Blood Flow (CBF). The perfusion is obtained from the difference between images with and without magnetic spin labeling of the arterial blood and the captured signal is around 0.5-2% of the magnitude of the labeling images, so the noise is one of the main problems for further data analysis. Classical method, *Mono-TI*, for CBF quantification is averaging repetitions with only one Inversion Time (TI) - the time delay between labeling and acquisition to allow the labeled blood to arrive the imaging slice. It improves the robustness to noise, however, cannot compensate the variety of Arterial Arrival Time (AAT). In this paper, *Diverse-TI* is proposed to exploit different TI sampling instants (sampling diversity) to improve the robustness to variety of AAT and simultaneously average repetitions with each TI (sampling repetitions) to improve the robustness to noise. Generally, the sampling diversity is relatively small and can be considered as compressed measurements, thus the Compressive Matched Filter (CMF) enlightened from sparsity is exploited to directly reconstruct CBF and AAT directly from compressed measurements. Meanwhile, regarding the CBF quantification performance, the compromise between the sampling repetition and sampling diversity is discussed and the empirical protocol to determine the sampling diversity is proposed. Simulations are carried out to highlight our discussions.

Key-words: Arterial Spin Labeling, Cerebral Blood Flow, Compressive Matched Filter, Diverse-TI, Diversity, Repetition

[*] Inria, VISAGES project-team, F-35042 Rennes, France
[†] University of Rennes 1, Faculty of medecine, F-35043 Rennes, France
[‡] INSERM, U746, F-35042 Rennes, France
[§] CNRS, IRISA, UMR 6074, F-35042 Rennes, France

Quantification du flux sanguin cérébral en ASL par Diverse-TI : diversité d'échantillonnage ou répétitions ?

Résumé : L'imagerie par marquage de spins artériels est une modalité d'imagerie par perfusion non-invasive qui permet la quantification absolue du flux sanguin cérébral (CBF). La perfusion est obtenue par soustraction de deux images : avant et sans marquage des spins artériels. Le signal capturé est alors d'environ 0.5-2% de l'amplitude du signal de chaque image. Le bruit est donc un des principaux problèmes. La méthode classique de quantification, *Mono-TI*, effectue la moyenne de plusieurs répétitions à un certain temps d'inversion (TI) correspondant au délai entre le marquage et l'acquisition. Cette moyenne améliore le rapport signal-sur-bruit, mais choisir un seul TI ne permet pas de prendre en compte les éventuelles variations du temps d'arrivée du bolus (AAT). Dans cet article, nous proposons une nouvelle technique, *Diverse-TI* , qui échantillonne à différents TI. Il s'agit alors de trouver un compromis entre la diversité d'échantillonnage et le nombre de répétitions par TI. En général la diversité d'échantillonnage reste relativement faible et on peut donc se placer dans le cadre d'acquisitions compressés (en anglais *compressed sensing*). La méthode *Compressive Matched Filter* (CMF) est donc utilisée pour estimer le CBF et l'AAT directement à partir des mesures. Concernant la quantification du CBF, le compromis entre la diversité d'échantillonnage et le nombre de répétitions par TI est discuté et un protocole expérimental est proposé.

Mots-clés : Marquage de spins artériels, flux sanguin cérébral, Compressive Matched Filter, diversité, répétition

1 Introduction

The Arterial Spin Labeling (ASL) is an MRI (Magnetic Resonance Imaging)-based perfusion technique which uses the magnetically tagged water as a freely diffusible tracer to measure perfusion non-invasive. This blood water is first labeled with a radio-frequency pulse in the neck of the patient. After a delay, called Inversion Time (TI), which allows the labeled blood to arrive in the brain, a labeled image of the brain is acquired. A control image is also acquired without labeling and the CBF estimation is done on the difference between the control and labeled image. For a fixed TI t, the perfusion signal is generally described by a kinetic model introduced by Buxton *et. al.* in [1]:

$$M_\Delta(t) = \begin{cases} 0, & t \in [0, \Delta) \\ 2\alpha f M_{0b}(t - \Delta)q_p(t)\exp(-t/T_{1b}), & t \in [\Delta, \Delta + \tau) \\ 2\alpha f M_{0b}\tau q_p(t)\exp(-t/T_{1b}), & t \in [\Delta + \tau, \infty) \end{cases} \tag{1}$$

where f is the CBF, α measures the labeling efficiency, M_{0b} is the equilibrium magnetization of arterial blood, Δ is the Arterial Arrival Time (AAT) to the interesting slice, τ is the temporal width of the bolus, T_{1b} is the relaxation time in blood and $q_p(t)$ is considered to be approximately equal to 1. Specifically, in QUIPSS II [2], a saturation pulse is given to the tagged bolus after a fixed period τ of the tagging time, thus the temporal width of the tagged bolus is known a priori.

The principal task of ASL analysis is quantifying the absolute value of CBF f. The traditional technique, which is called *Mono-TI*, only uses a single TI t after which the acquisition is gathered, where t is assumed to be bigger than $\Delta + \tau$ to guarantee a delay long enough to let the magnetic tagged blood arrive the interesting imaging slice. Then the quantification of CBF is a direct ratio between the magnetization difference M_Δ and the known terms, when $t > \Delta + \tau$.

However, two major problems prevent the efficiency of Mono-TI. At first, as the amplitude of the difference ASL signal is usually around 0.5-2% of the control image magnitude, its SNR is thus not sufficient for further analysis. Commonly, numbers of sampling repetitions are acquired for single TI (typically more than 30) and then averaged to improve the SNR. Secondly, the assumption $t > \Delta + \tau$ is not easy to be guaranteed in Mono-TI technique. Since Δ is varying between different patients, ages and physical situations. Even excluding these factors, the AAT is still an uncertain value due to the presence of laminar and turbulence flow, complicated vessel networks and cardiac pulsations [3]. This fact leads that the magnetic labeled blood may not have reached the imaging slice if the sampling time is too small and thus leads to underestimation of CBF. One possible way is giving the TI large enough, however, the magnetization difference M_Δ might be too small if TI is too big and thus leads to very low SNR.

In this paper, another measuring procedure with different sampling times is investigated for the CBF quantification, where the collected ASL data at different sampling times are captured during separate ASL RF pulse periods. It is different from the classical *Multi-TI* [4, 5, 6] and thus called *Diverse-TI* to avoid ambiguities. Multi-TI is a more recent and confidential sequence than Mono-TI and is not currently available on most MR-Scanners, while Diverse-TI proposed in this paper can easily be produced since it only uses regular ASL sequences. Before further analysis on real ASL data, the first and also the essential step is giving a protocol to concretely design the measuring procedures. It is clear that some issues should be preferentially considered: (1) *sampling repetition* (for the same sampling time), which is intended to improve SNR; (2) *sampling diversity* (sampling at different times) which is intended to compensate for the inexact knowledge of parameters such as Δ, etc. For practical considerations, the most crucial criteria in real clinical studies is the *total measuring time* which is generally limited in a reasonable period.

Thus the values of sampling repetition and sampling diversity can not be designed as large as possible to improve CBF quantification performance. A method to explicitly guide the design of these parameters is applaudable. However, to the best knowledge of the authors, the existing papers rarely focus on this point.

Consequently, as a preliminary study, the contribution of this paper is twofold. First, it formulates the considered problem as an instance of Compressive Matched Filter (CMF) [7]. Then, it numerically investigates the trade-offs between repetition and sampling diversity (for the same total measurement time) on CBF estimation with CMF. In a word, the main question investigated in this paper is: given a total measurement time, shall we favor repetitions or sampling diversity?

2   Diverse-TI Technique

Since parameters including $\tau, T_{1b}, \alpha, M_{0b}$ and $q_p(t)$ are (or assumed to be) known a priori, the signal model (1) can be simplified as $M_\Delta(t) = f \times g(\Delta; t)$ where the time related term $g(\Delta; t)$ will be called "wave form" and can be defined by (1) with $f = 1$.

- Sampling Repetition
In practice, an important level of noise is affecting ASL measurements, hence the signal captured at time t can be expressed as follows:

$$y(t) = M_\Delta(t) + \epsilon(t) = f \times g(\Delta; t) + \epsilon(t)$$

where $\epsilon(t)$ is the noise term and is assumed to be Gaussian in this paper. In our setting, the measure at time t is repeated R times (sampling repetition), and averaging all measures divides the noise variance by R and thus it will improve the SNR according to the following equation:

$$Q_R = 10 \log_{10} R + Q_1 \tag{2}$$

where Q_1 is the SNR of one repetition and Q_R is the SNR after R repetitions.

- Sampling Diversity
Define $\boldsymbol{g}(\Delta) = \{g(\Delta, iT_s)\}_{i=1}^N$ where T_s is a reference regular sampling interval and $t_1...t_M$ (possibly irregular) time instants located on this regular grid, where $M \ll N$. With different TI (sampling diversity) $t_1...t_M$, the ASL data are respectively collected $\boldsymbol{y} \triangleq \{y(t_1), ..., y(t_M)\}^T \in \mathbb{R}^M$. Then we can write the sampling model in the form of linear operation:

$$\boldsymbol{y} = \Phi(f \times \boldsymbol{g}(\Delta) + \boldsymbol{\epsilon})$$

where $\Phi \in \mathbb{R}^{M \times N}$ is a sensing matrix, which verifies $\Phi\Phi^T = \boldsymbol{I}_M$.

At last, the task is to find the CBF parameter f and the optimal Δ that best match the observations $\boldsymbol{y}$. To fulfill it, Compressive Matched Filter (CMF) [7] is exploited in the following sections.

3   Compressive Matched Filter

In the case considered in this paper, the CBF quantification problem can be formed as a multiple detection problem to distinguish the following hypothesis:

$$\mathcal{H}_i : \boldsymbol{y} = \Phi(f\boldsymbol{g}(\Delta_i) + \boldsymbol{\epsilon}), \text{ with } i \in \{1, ..., d\}$$

where f is the CBF value, $\Delta_1, ..., \Delta_d$ are d possible AAT values that should be assumed before and $\boldsymbol{\epsilon} \sim \mathcal{N}(0, \sigma^2 \boldsymbol{I}_N)$ is the white noise term. In this case, the evidence under different hypothesis, for $i \in \{1, ...d\}$, can be written

$$p(y|\mathcal{H}_i) = \frac{\exp\left(-\frac{1}{2}(\boldsymbol{y} - \Phi f \boldsymbol{g}(\Delta_i))^T (\sigma^2 \Phi\Phi^T)^{-1}(\boldsymbol{y} - \Phi f \boldsymbol{g}(\Delta_i))\right)}{(2\pi)^{N/2}|\sigma^2 \Phi\Phi^T|^{1/2}}$$

Then the final detection is carried out by finding the hypothesis with the biggest conditional probability:

$$(f_s, \mathcal{H}_s) = \underset{f, \mathcal{H}_i, i\in\{1,...,d\}}{\arg\max} \, p(y|\mathcal{H}_i)$$

Thus by differentiating w.r.t. f, we can obtain its estimation

$$\hat{f}_i = \frac{\boldsymbol{y}^T (\Phi\Phi^T)^{-1} \Phi \boldsymbol{g}(\Delta_i)}{\boldsymbol{g}(\Delta_i)^T \Phi^T (\Phi\Phi^T)^{-1} \Phi \boldsymbol{g}(\Delta_i)} \tag{3}$$

and by taking logarithm we obtain an equivalent test that simplifies to

$$
\begin{aligned}
\mathcal{H}_s &= \underset{\mathcal{H}_i, i\in\{1,...,d\}}{\arg\max} \, \left(\boldsymbol{y} - \frac{1}{2}\Phi\hat{f}_i\boldsymbol{g}(\Delta_i)\right)^T (\Phi\Phi^T)^{-1} \Phi\hat{f}_i\boldsymbol{g}(\Delta_i) \\
&= \underset{\mathcal{H}_i, i\in\{1,...,d\}}{\arg\max} \, \frac{1}{2}\frac{\left(\boldsymbol{y}^T(\Phi\Phi^T)^{-1}\Phi\boldsymbol{g}(\Delta_i)\right)^2}{\boldsymbol{g}(\Delta_i)^T\Phi^T(\Phi\Phi^T)^{-1}\Phi\boldsymbol{g}(\Delta_i)} \\
&\overset{\Phi\Phi^T=I}{=\!=\!=\!=} \underset{\mathcal{H}_i, i\in\{1,...,d\}}{\arg\max} \, \left|\left\langle \boldsymbol{y}, \frac{\Phi\boldsymbol{g}(\Delta_i)}{\|\Phi\boldsymbol{g}(\Delta_i)\|_2} \right\rangle\right|
\end{aligned}
\tag{4}
$$

Above all, using (4) and (3), we can respectively obtain the estimation of arrival time $\hat{\Delta} = \Delta_s$ and the estimation of CBF $\hat{f} = f_s$.

4   Mono-TI technique v.s. Diverse-TI technique

In fact, $M = 1$ is exactly the Mono-TI technique. In order to well illustrate the performance of Mono-TI technique, a concrete simulation is carried on. In the following, the parameters of ASL model (1) are arbitrarily set as: $M_{0b} = 100, \alpha = 0.9, T_{1b} = 1.2s$ and $\tau = 1s$, and Fig. 1(left) shows one example when AAT $\Delta = 1$ and CBF $f = 10$ mL/(100g)/min. Obviously, given constant noise variance σ, the highest SNR of single repetition Q_1 is reached when $t_i = \Delta + \tau$ while it will decrease as t_i increasing.

The assumption on TI $t_i > \Delta + \tau$ is supposed to be verified. At first, t_i can not be much smaller than $\Delta + \tau$ otherwise the tagged blood can not reached the interesting slice on time, as shown by the red diamond point in Fig. 1(left) when $t_i = 1s$; meanwhile, it can not be too big otherwise the captured signal will be too small which makes the SNR Q_1 very low, as shown by the green circle point in Fig. 1(left) when $t_i = 4.5s$. Then the CBF f can be calculated directly by $\hat{f} = y(t_i)/g(\Delta; t_i)$, however, the AAT Δ can not be estimated in Mono-TI technique.

Then Mono-TI technique is carried out in the following procedure. Fix the CBF $f = 10$ mL/(100g)/min, give one AAT value Δ, sample at the time t_i with noise corruption, and then one single repetition of the ASL signal is simulated. Without loss of generality, the time used for one single repetition is assumed $T_S = 5s$ (this value is set identically for all simulations). Then as an example, we can set the total time $T = 30$min, so according to (5) the Mono-TI technique allows $R = 360$ repetitions. According to (2), the SNR can reach to $Q_R = 30.56dB$

with $Q_1 = 5dB$. However, this value is very sensible to the sampling location, or equivalently, the AAT value. This fact can be well illustrated by Fig. 1, where the result of Mono-TI is obtained by fixing $t_i = 1s$, $3s$ or $4.5s$, then ranging AAT Δ from $0.1s$ to $3s$ (the performance shown in Fig. 1(right) is measured through the quantification SNR averaged over 1000 restarts). In Fig. 1, the result when $t_i = 1s$ shows the situation when TI is too short, $t_i = 4.5s$ shows the situation when TI is too long, even with proper TI $t_i = 3s$, the performance of quantification might largely decrease when AAT and the TI are mismatch.
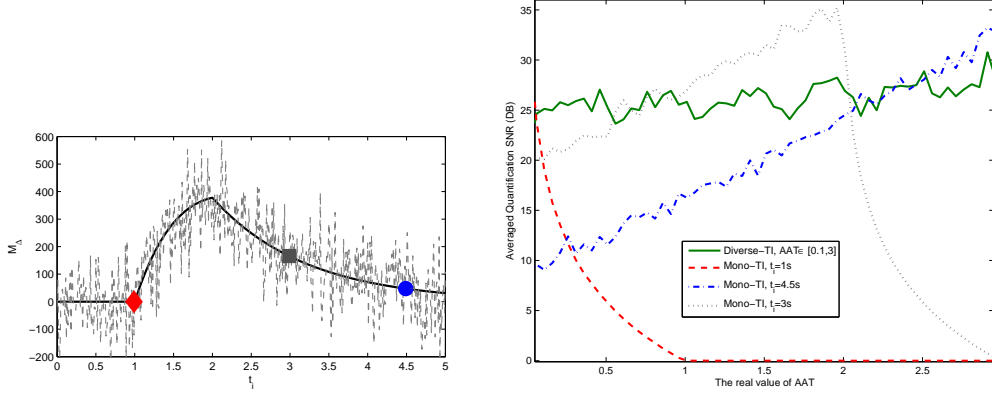

Figure 1: (Top) Kinetic Model of ASL with $\Delta = 1$ ($\tau = 1s$) and $f = 10$ mL/(100g)/min (dark solid curve) and its noisy version with average SNR $5dB$ (grey dashed curve). (Bottom) Comparison between Mono-TI and Diverse-TI ($M = 10$) methods for different AAT with total time $T = 30$.

In the framework of Diverse-TI , following the CMF algorithm, we first assess a large interval where the value of AAT should locate. In this simulation, this interval is set to $\Delta \in [0.1, 3]$. We choose the number[1] of sampling diversity to $M = 10$, and the sampling repetitions are set identically according to (5) with the same total measuring time as Mono-TI, then the CBF quantification performances through CMF algorithm with different AAT value are obtained, as shown in Fig. 1. Diverse-TI can give constant performance which is also better than Mono-TI with a majority of AAT.

As a conclusion, in the case of $M = 1$, the CBF quantification quality might be better than $M > 1$, however, its performance is much sensitive to the sampling time, which is not easy to be designed practically. Moreover, as a supplement, Diverse-TI can also estimate the AAT.

5   Experiments and simulations

Without loss of generality, the time used for one single sampling repetition can be assumed to be T_S, including the process of one time control imaging and tagging imaging. Then the total measuring time can be expressed as:

$$T \propto M \cdot R \cdot T_S \tag{5}$$

where M indicates the level of sampling diversity i.e. the number of TI and R the number of sampling repetitions. For practical considerations, the most crucial criteria in real clinical

---

[1]This value is chosen according to empirical result, referring Fig. 2.

studies is the total measuring time which is generally limited in a reasonable period. In one aspect, the sampling repetitions improve the signal SNR; while in the other aspect, the sampling diversity promote the robustness to the variety of AAT. Consequently, the compromise between the sampling diversity and sampling repetitions needs to be determined. In other words, given the maximum total time T, how to optimally choose R and M to reach better CBF quantification?

5.1 Acquisition

A healthy volunteer was scanned on QUIPSS II with image size 64×64 and the volume size $3 \times 3 \times 4mm$. Fourteen slices were acquired with TIs for the lowest slice $TI_1/\Delta TI/TI_N = 1200ms/100ms/2200ms$ and an extra delay of $45ms$ between slices, i.e. with diversity $M = 11$. Meanwhile, 40 repetitions (control-labeled pairs) for each TI were captured, i.e. with repetitions $R = 40$. All 40 repetitions were co-registered to compensate for the patient motion with the first one using 3D rigid-body transformation implemented in SPM-Toolbox.

To estimate the CBF and AAT, the parameters in the perfusion model to the sequence of Diverse-TI difference images are set according to the most used in the literatures: tissue relaxation time $T_1 = 900ms$, blood relaxation time $T_b = 1500ms$, blood-tissue ratio coefficient $\lambda = 0.9$ and the magnetization efficiency $\alpha = 0.9$. The time width of the labeled blood in QUIPSS II is fixed as $\tau = 700ms$.

5.2 Performance Assessment

The performance assessment to simulations can be easily calculated by referring the ground truth of CBF or AAT, and then the quantification SNR for CBF and AAT can be defined:

$$Q_f(M, R) = 20 \log_{10} \frac{\|f_{true}\|}{\|\hat{f}(M, R) - f_{true}\|}$$

and

$$Q_\Delta(M, R) = 20 \log_{10} \frac{\|\Delta_{true}\|}{\|\hat{\Delta}(M, R) - \Delta_{true}\|}$$

with $\hat{f}(M, R)$ the estimation of CBF when diversity is M and repetition is R, and f_{true}, Δ_{true} are respectively the groundtruth of CBF and AAT. It is worth mentioning that, instead of voxel-wised SNR, the quantification SNRs (both for CBF and for AAT) are computed over the whole perfusion images.

However, the ground truth is not available for real data, and thus an approximation to the ground truth is computed from all available data ($M = 11$ and $R = 40$) using CMF. Then the performance are assessed regarding to the approximated ground truth, noted by $f_{all} = \hat{f}(11, 40)$ and $\Delta_{all} = \hat{\Delta}(11, 40)$. At the end, the performance assessment for CBF quantification with the real data is carried out by calculating the following reconstruction SNR:

$$Q_f(M, R) = 20 \log_{10} \frac{\|f_{all}\|}{\|\hat{f}(M, R) - f_{all}\|}$$

Accordingly, for AAT:

$$Q_\Delta(M, R) = 20 \log_{10} \frac{\|\Delta_{all}\|}{\|\hat{\Delta}(M, R) - \Delta_{all}\|}$$

Remark 5.1 *Although the approximated ground truth can not perfectly represent the real ground truth, we can still assume that the expected quantification with more data will be closer to the real ground truth than that estimated from less data.*

5.3 Sampling diversity and repetitions with random sampling locations

In section 4, it has been shown that $M = 1$ is worse than $M > 1$, while in this subsection, we will propose a method to answer the question that how many sampling time locations are enough? Similarly, the total time T is the crucial parameter in clinical studies. Consequently, given a fixed total time T, the relationship between the CBF quantification performance and the number of sampling locations is essential to determine the required M.

In this simulation, the CBF f is fixed equal to $10\mathrm{mL}/(100\mathrm{g})/\mathrm{min}$ and the AAT Δ is randomly choosing from the interval $[0.1, 2]$, then the ASL signal are generated and corrupted by noises. Then to simulate the sampling procedure, the total time T is fixed respectively to $5, 10, 30, 60\mathrm{min}$ and the number of sampling time locations M is varying from 2 to 30, thus the number of repetitions R is determined via (5), then samples are collected. Since $\Delta \in [0.1, 2]$ is assumed, the CMF can be used to carry out the CBF quantification and AAT estimation, and the SNR of CBF quantification and AAT estimation are respectively shown in Fig. 2 (b) and (c). Meanwhile, the relationship between sampling repetition and sampling diversity can also be drawn according to (5), as shown in Fig. 2 (a).
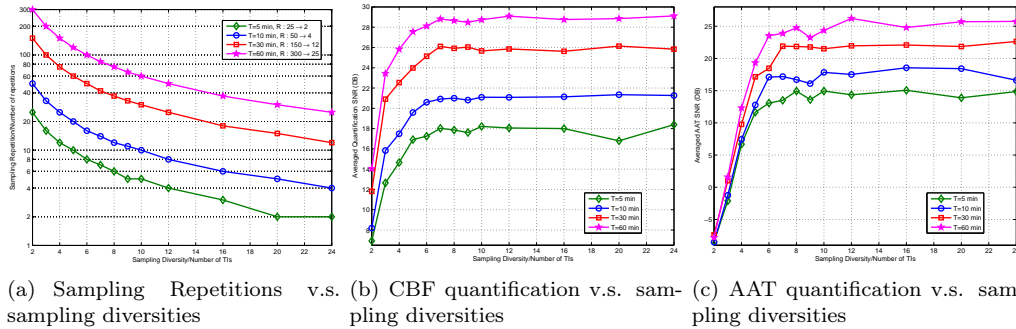

(a) Sampling Repetitions v.s. sampling diversities

(b) CBF quantification v.s. sampling diversities

(c) AAT quantification v.s. sampling diversities

Figure 2: Performance Evolution with respect to different sampling diversities M via CMF using different total time.

From the results, as expected, we can find that as M increases, the performance of Diverse-TI technique is improving before reaching an asymptotic value. From this simulation, we can find that the convergent point is around $M = 8$, as shown by the performance of CBF (or AAT) quantification in bottom figures of Fig. 2. Then according to (5), the repetitions at one sample time R can be calculated. It is worth mentioning that this simulation is only an example of choosing the number of multiple sampling time locations, for concrete applications, the curve in Fig. 2 should be re-drawn with appropriate parameters, and then the best value should be re-selected.

5.4 Best Sampling Locations

From the perfusion model, the perfusion signal magnitude has a peak at some time position. Assuming that the measuring model is Gaussian, one can find that the measuring SNR will be

the highest at the peak position and thus give the best reconstruction performance for CBF. On the other hand, the estimation of arrival time Δ is very sensitive to the first sampling point, for instance $\boldsymbol{y}(1) = 0$ and $\boldsymbol{y}(1) \neq 0$ will give very different results for Δ. Consequently, to eliminate the influence of the sampling locations, we first determine the best sampling locations, where the samples will give the best performance at each diversity and repetition level.

In this experiment, the estimations are obtained from all possible combinations of sampling positions at every sampling diversity, for instance, when $M = 2$, it will have $\binom{11}{2}$ possible sampling patterns. Then we can choose the best sampling locations as the sampling patterns with the best estimation performance, either for CBF or for AAT. The results are listed in Tab. 1.

Table 1: The best sampling locations. The relation between location index and sampling time is shown in Tab. 2.

M	Best for CBF	Best for AAT	CBF & AAT
2	5,10	2,9	2,9
3	2,5,10	2,7,11	2,6,11
4	2,6,8,11	2,5,7,11	2,6,7,11
5	3,5,6,8,11	1,5,7,9,11	1,5,6,8,11
6	3,6,8,9,10,11	1,5,6,7,9,11	1,6,7,9,10,11
7	3,6,7,8,9,10,11	1,3,5,7,8,9,11	1,3,6,7,9,10,11
8	3,5,6,7,8,9,10,11	1,3,4,6,7,8,9,11	1,3,6,7,8,9,10,11
9	1,3,5,6,7,8,9,10,11	1,3,5,6,7,8,9,10,11	1,3,5,6,7,8,9,10,11
10	1,2,3,5,6,7,8,9,10,11	1,3,4,5,6,7,8,9,10,11	1,2,3,4,6,7,8,9,10,11

Table 2: Location index and its corresponding sampling time.

Location Index	Sampling Time (seconds)
1	1.2
2	1.3
$\vdots$	$\vdots$
11	2.2

To make a compromise between the best sampling locations for CBF and for AAT, we consider the following value as the criterion:

$$Q_{f+\Delta} = Q_f + Q_\Delta$$

Then choose the biggest $Q_{f+\Delta}$ to determine the best sampling locations both for CBF and AAT, as shown in the last column in Tab. 1.

Remark 5.2 *Considering the results listed in Tab. 1, we can get another table by counting the number of time locations selected as the best sampling locations, as shown in Tab. 3. From Tab. 3, we can conclude that in order to obtain better performance, the optimal way to choose the sampling time positions are the following: first capture a sample at the starting point, then some samples in the middle and one sample at the end.*

In the following experiments, we will fix the sampling locations following the best sampling locations shown in the last column of Tab. 1 for each diversity level, then investigate the effects of different repetitions.

Table 3: Number of time locations selected as the best sampling locations.

Time Locations	1	2	3	4	5	6	7	8	9	10	11
For CBF	2	3	6	0	6	7	4	7	5	7	7
For AAT	6	3	4	2	6	4	8	4	7	2	8
CBF & AAT	6	4	4	1	2	8	6	4	6	5	8

5.5   Performance Evaluation Map with Best Sampling Locations

In section 5.3, we have discussed that the level of diversity can be determined according to the performance evolution curves, as shown in Fig. 5. And from the result, we can easily assess the optimal diversity and optimal repetitions for a given total measuring time. In this section, we will turn to use the performance evolution map to determine an optimal compromise, where we can find the optimal diversity or repetitions much easier.

5.5.1   Experiments on simulated data

In order to make the simulated data much closer to the real case, we first generate the AAT values from the estimation of AAT from real perfusion data, as shown in Fig. 3. Then the simulated perfusion signals are generated with the generated AAT and a fixed CBF value (it is set to 80 here). Thus for each level of diversity, the best TIs are chosen from Tab. 1, which means part of the data has been used to estimate the CBF and AAT. Meanwhile, different levels of noises are added with respect to different level of repetitions, and the values of noise SNR can be referred by (2). Then CMF is exploited to do the CBF and AAT quantification, for every level of diversity and every level of repetition. And the quantification SNRs of each level of diversity and repetitions for CBF $Q_f(M, R)$ and for AAT $Q_\Delta(M, R)$ can then be calculated. Finally, we re-run the simulations 100 times with different draw of noises, and correspondingly, 100 quantification SNRs for CBF and for AAT are obtained, respectively denoted by $Q_f^{(1)}(M, R), ..., Q_f^{(100)}(M, R)$ and $Q_\Delta^{(1)}(M, R), ..., Q_\Delta^{(100)}(M, R)$. Then the mean value of the quantification SNR for CBF and for AAT can be calculated as following:

$$\bar{Q}_f(M, R) = \frac{1}{100} \sum_{i=1}^{100} Q_f^{(i)}(M, R)$$

$$\bar{Q}_\Delta(M, R) = \frac{1}{100} \sum_{i=1}^{100} Q_\Delta^{(i)}(M, R) \tag{6}$$

And the map of $\bar{Q}_f(M, R)$ and $\bar{Q}_\Delta(M, R)$ are respectively shown in Fig. 4 (a) and (c).

Meanwhile, the standard variation of the quantification SNR for CBF and for AAT can also be calculated as following:

$$\tilde{Q}_f(M, R) = \sqrt{\frac{1}{100} \sum_{i=1}^{100} (Q_f^{(i)}(M, R) - \bar{Q}_f(M, R))^2}$$

$$\tilde{Q}_\Delta(M, R) = \sqrt{\frac{1}{100} \sum_{i=1}^{100} (Q_\Delta^{(i)}(M, R) - \bar{Q}_\Delta(M, R))^2} \tag{7}$$

And the map of $\tilde{Q}_f(M, R)$ and $\tilde{Q}_\Delta(M, R)$ are respectively shown in Fig. 4 (b) and (d).

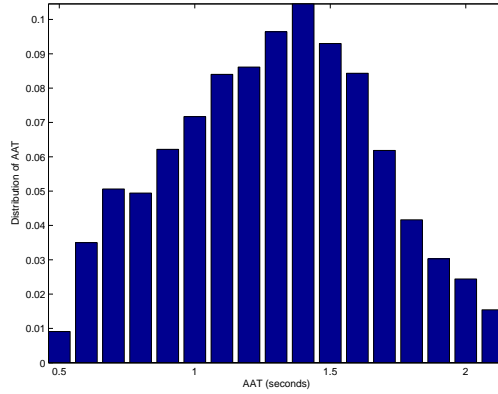Figure 3: The distribution of estimated AAT from real perfusion data.

(a) Mean of SNR for CBF   (b) Standard variation of SNR for CBF

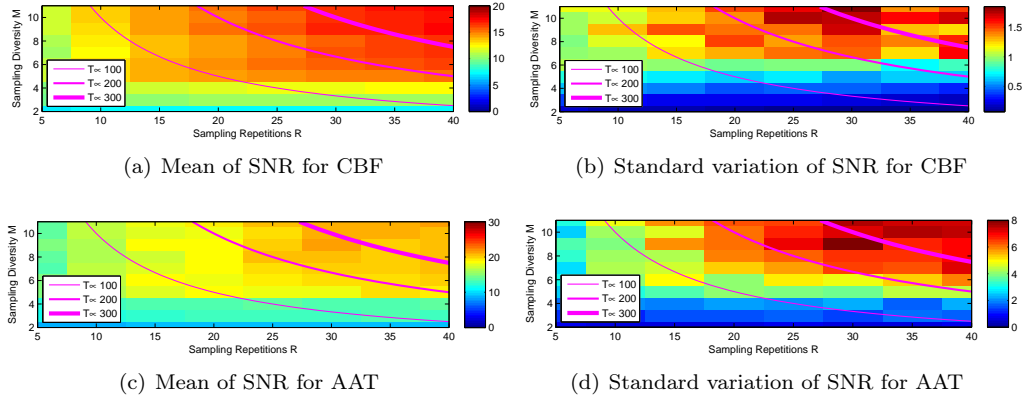(c) Mean of SNR for AAT   (d) Standard variation of SNR for AAT

Figure 4: The performance evaluation map with best sampling locations on simulated perfusion data.

After that, we can then plot the isoheight of the total measuring time for different diversity and repetitions. As shown in Fig. 4, three isoheight curves are given respectively to $T \propto 100, 200, 300$.

First, we can focus on the mean value of the quantification SNR for CBF and AAT, and we can find that the results are similar to the results presented in section 5.3. The conclusion of both results is that a diversity M around 5 can give similar results as when the diversity M much bigger. One more conclusion from Fig. 4 is that the performance will drop down when the sampling repetitions are decreasing.

Secondly, let us focus on the standard variation of the quantification SNR for CBF and AAT. For CBF, as shown in Fig. 4 (b), the variation is much lower when the diversity $M \leq 5$. While for AAT, as shown in Fig. 4 (d), the sharp transition of variation appears when the diversity M is from 5 to 4. It is shown that the lower diversity gives the more robust quantification both for CBF and AAT.

Above all, we can conclude from the simulated results that the best diversity level is $M = 5$, and then the corresponding repetition level can be chosen according to the total measuring time T.

Remark 5.3 *One abnormal phenomenon is that lower diversity gives more robust quantification*

for fixed repetitions. It is due to the reason that even though higher diversity indeed improves partial of the voxels, there still exist lots of voxels of which the performance cannot be improved by only increasing the diversity. On the other hand, the performances with low diversity for all voxels are low. Consequently, increasing the diversity might increase the variation of the quantification SNR.

Another abnormal phenomenon is that the variation of the SNR for AAT is increasing as increasing the repetitions for fixed diversity. It is due to the fact that for fixed diversity, by increasing repetitions can improve the performance for some of the voxels, while others do not change to much. Thus the average SNR is increasing while the standard variation is also increasing.

5.5.2   Experiments on real data

(a) Mean of SNR for CBF

(b) Standard variation of SNR for CBF

(c) Mean of SNR for AAT

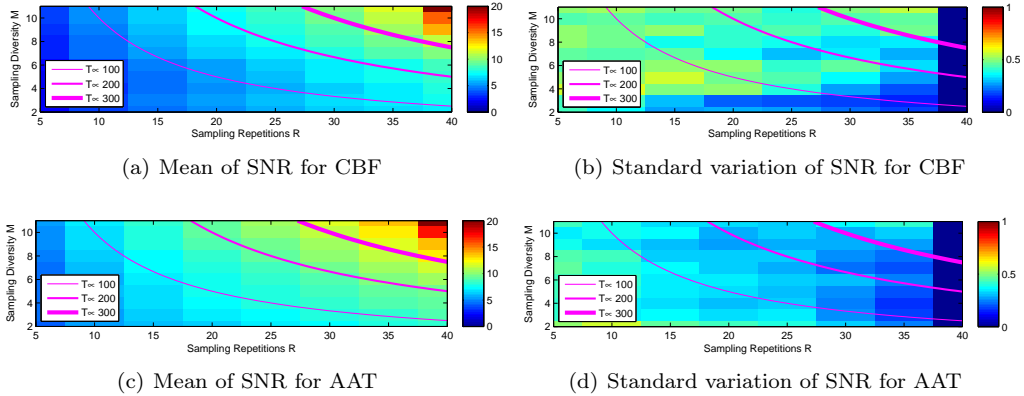(d) Standard variation of SNR for AAT

Figure 5: The performance evaluation map with best sampling locations on real perfusion data.

In this subsection, we will use the similar procedure to obtain the performance evaluation map for real data. It is worth claiming that the references of CBF and AAT of real data are their quantifications by using all data, i.e. the quantification when $M = 11$ and $R = 40$.

Then the one-running process i is described as following: Firstly, the sampling locations for each diversity level are determined by the best TIs for both CBF and AAT, as shown in Tab. 1. Denote Ω the set of index of sampling repetitions, thus $\Omega = \{1, ..., 40\}$. Then for repetition level R, there will be $P(R) = \binom{|\Omega|}{R}$ different selections and the selected samples are randomly chosen from the set Ω. After that, the quantification of CBF and AAT can be calculated by CMF for different diversity levels and repetition levels, i.e. $Q_f^{(i)}(M, R)$ and $Q_\Delta^{(i)}(M, R)$. Finally, we re-do the one-running process 100 times with randomly selection of repetitions, i.e. i is ranging from 1 to 100. The performance evaluation map can be obtained by averaging the quantification SNR according to (6) and calculating its standard variation according to (7), as shown in Fig. 5. In addition, the CBF and AAT quantifications from real data with different diversity and repetition levels are given in Fig. 6.

The first impression of the performance evolution maps for real data (shown in Fig. 5) and the simulated data (shown in Fig. 4) is that there exist lots of differences:

- Fixing the repetition level, for real data, increasing the diversity will always improve the average SNR for both CBF and AAT; while for simulated data, the average SNR will
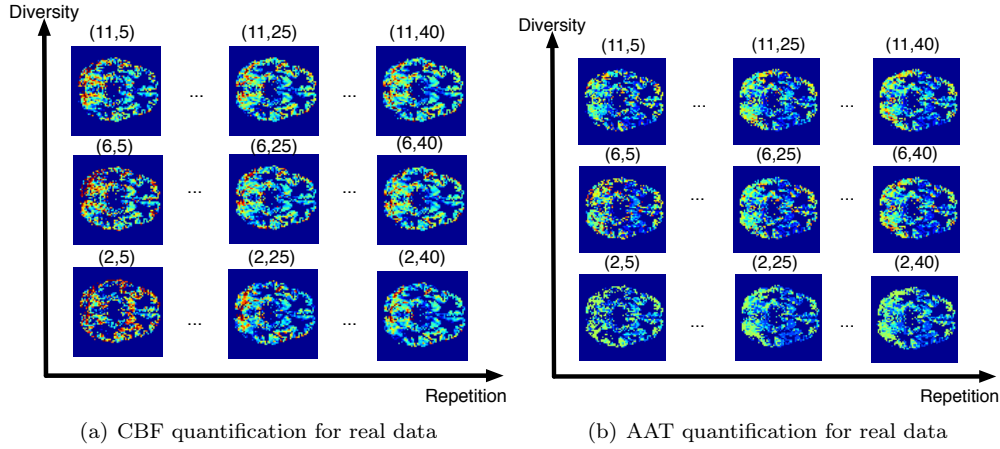
(a) CBF quantification for real data

(b) AAT quantification for real data

Figure 6: The estimated CBF and AAT maps from real data corresponding to different diversity and repetition levels (M, R).

increase until the diversity reaches $M = 5$ then stays almost constant as increasing the diversity.

- Considering the standard variation of performance SNR for AAT, for real data, increasing repetition level will decrease the variation; while for simulated data, the variation is increasing (in general) as increasing the repetition level.

For the first difference, it is due to the fact that the Buxton's model used here is not proper for the real data, as shown in Fig. 7. We first generate the perfusion signal with Harbe's model with Gaussian distribution, then the Buxton's model is exploited for CBF and AAT quantification by CMF. The resulted performance evaluation map (Fig. 7) is very similar to those of the real data (Fig. 5). In other words, we can also conclude from the results that Buxton's model is not precise for the real perfusion data.

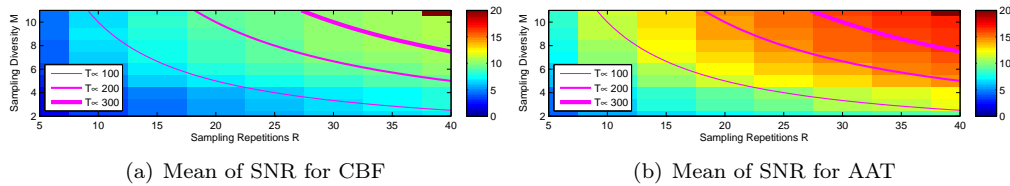(a) Mean of SNR for CBF

(b) Mean of SNR for AAT

Figure 7: The performance evaluation map when the perfusion models used for generating data and used for quantification are mismatch.

The reason of the second difference is because of the following. The value $\binom{|\Omega|}{R}$ is varying as increasing the repetitions and if the number of re-running times are bigger than $P(R)$, there will exist some identical selections from Ω and thus it will influent the standard variation map. Particularly, the variation when $R = 40$ will equal to 0.

Unfortunately, the results from the real data can not clearly give any clues on determining the compromise between diversity level and repetition level under fixed total measuring time.

6   Discussion and Conclusion

In this report, we first introduced the Diverse-TI, which exploits samples at multiple TIs to quantify the CBF and AAT. Many repetitions are required for each TIs sampling point to improve the data fidelity. Then the question is how many repetitions and how many TIs should we determine to get as highest performance as possible? In this report, we proposed to use the performance evaluation map to determine the compromise between the diversity level and the repetition level.

The simulated results can clearly give us the best way for design the diversity level and the repetition level. The best diversity level is $M = 5$, and then the corresponding repetition level can be chosen according to the total measuring time T.

The performance evaluation map from the real data can show us that increasing either diversity or repetitions can improve the performance. However, it cannot clearly give us any clues on the compromise of the diversity level and the repetition level.

Even though the performance evaluation map can give us some clues on designing the sampling procedure for Diverse-TI, the relationships between the ultimate results and the following aspects are still unclear and need further investigations: *quantification algorithm, approximated references* and *perfusion model*.

6.1   The relation with the exploited quantification algorithm

In this report, we did not analyze the performance of quantification algorithm, i.e. CMF, which is assumed to be good enough here to fulfill the quantification. In fact, many algorithms can be exploited here. Consequently, corresponding to different quantification algorithms, the resulted performance evaluation maps might be different, but it will not completely change the evaluation map. Thus the variation with respect to different algorithms requires further investigations and we believe that using the similar procedure, one can get it's performance evaluation map, with which the compromise between diversity and repetitions can be optimally determined.

6.2   The relation with the approximated references

In fact, the reference (the ground-truth) of the CBF and AAT in real world is unknown. Consequently, instead of the ground-truth, the approximated reference estimated from the full data set is exploited in the experiments. However, the fidelity of the approximated reference is not investigated in this report. In fact, the approximated reference exploited here can be assumed to be close to the ground-truth. Even though the error introduced by the approximated reference inherently exists, comparing to the quantification error arisen by reducing the sampling diversity or repetitions, this error is relatively small and thus the corresponding performance evaluation map will not change too much. Fig. 8 presents the performance evaluation map using the approximated reference for simulated perfusion data. Comparing to Fig. 4, we can find that the results obtained with the approximated reference are similar to the results with the correct ground-truth and the similar conclusion on the comprise between diversity and repetition can be made. Consequently, in some sense, it shows that the approximated reference does not influent too much on the final result.

6.3   The relation with the perfusion model

The last issue is about the perfusion signal model. As shown by the mismatch of the results between simulation and reality, we found that the misuse of the perfusion signal model will

(a) Mean of SNR for CBF

(b) Standard variation of SNR for CBF

(c) Mean of SNR for AAT

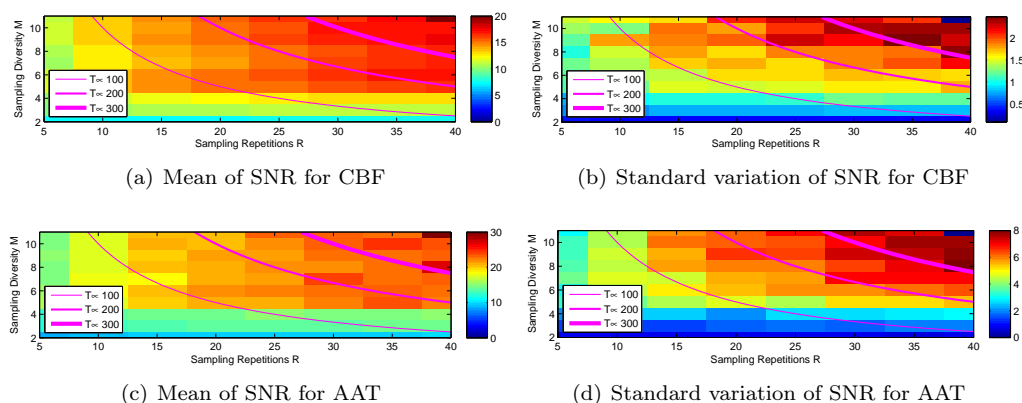(d) Standard variation of SNR for AAT

Figure 8: The performance evaluation map obtained with best sampling locations and with approximated references on simulated perfusion data.

lead very different performance evaluation maps. Consequently, it is better to use more precise perfusion signal model for the real data.

As a conclusion, we proposed a simple multi-TIs sampling procedure for ASL, Diverse-TI, which is superior to the Mono-TI method. Meanwhile, the performance evaluation map is proposed to determine the diversity level and repetition level in the Diverse-TI framework. Although we can not easily find the optimal compromise between diversity and repetition by using the performance evaluation map from the real data, the simulated results give us some clues on designing the two essential parameters.

References

[1] R B Buxton, L R Frank, E C Wong, B Siewert, S Warach, and R R Edelman. A general kinetic model for quantitative perfusion imaging with arterial spin labeling. *Magnetic resonance in medicine : official journal of the Society of Magnetic Resonance in Medicine / Society of Magnetic Resonance in Medicine*, 40(3):383–96, September 1998.

[2] W M Luh, E C Wong, P a Bandettini, and J S Hyde. QUIPSS II with thin-slice TI1 periodic saturation: a method for improving accuracy of quantitative perfusion imaging using pulsed arterial spin labeling. *Magnetic resonance in medicine : official journal of the Society of Magnetic Resonance in Medicine / Society of Magnetic Resonance in Medicine*, 41(6):1246–54, June 1999.

[3] Wen-Chau Wu, Yousef Mazaheri, and Eric C Wong. The effects of flow dispersion and cardiac pulsation in arterial spin labeling. *IEEE transactions on medical imaging*, 26(1):84–92, January 2007.

[4] Reinoud P H Bokkers, Jochem P Bremmer, Bart N M van Berckel, Adriaan a Lammertsma, Jeroen Hendrikse, Josien P W Pluim, L Jaap Kappelle, Ronald Boellaard, and Catharina J M Klijn. Arterial spin labeling perfusion MRI at multiple delay times: a correlative study with H(2)(15)O positron emission tomography in patients with symptomatic carotid artery occlusion. *Journal of cerebral blood flow and metabolism*, 30(1):222–229, January 2010.

[5] B J MacIntosh, a C Lindsay, I Kylintireas, W Kuker, M Günther, M D Robson, J Kennedy, R P Choudhury, and P Jezzard. Multiple inflow pulsed arterial spin-labeling reveals delays in the arterial arrival time in minor stroke and transient ischemic attack. *AJNR. American journal of neuroradiology*, 31(10):1892–4, November 2010.

[6] Jiongjiong Wang, Daniel J Licht, Geon-Ho Jahng, Chia-Shang Liu, Joan T Rubin, John Haselgrove, Robert a Zimmerman, and John a Detre. Pediatric perfusion imaging using pulsed arterial spin labeling. *Journal of magnetic resonance imaging : JMRI*, 18(4):404–13, October 2003.

[7] Mark A Davenport, Student Member, Petros T Boufounos, Michael B Wakin, and Richard G Baraniuk. Signal Processing With Compressive Measurements. *IEEE Journal of Selected Topics in Signal Processing*, 4(2):445–460, 2010.